Webology (ISSN: 1735-188X)
Volume 19, Number 2, 2022

Experimental Investigation And Modeling Specific Wear Rate Of AISI 304 Using Response Surface Methodology

Dler A. Ahmed[1] , Mohammedtaher M. Mulapeer[2]

[1]Department of Mechanical and Mechatronics, College of Engineering, Salahaddin University–Erbil, College of Engineering, Erbil, Iraq.

[2]Department of Mechanical and Mechatronics, College of Engineering, Salahaddin University–Erbil, College of Engineering, Erbil, Iraq.

Abstract

In this work, the design of the experiment was used to study the influences of temperature, applied load, and sliding speed on the specific wear rate (SWR) of AISI 304 under a dry sliding pin on a disc experiment. It is found that the experimental SWR increased with the increase of temperature and sliding speed up to a certain value and then decreased significantly. It varied linearly with the applied load. In addition, the morphology of the worn surfaces was illustrated by scanning electron microscope (SEM) and the prospect of oxide layer formation due to friction and heat was inspected by x-ray diffraction (XRD). Furthermore, response surface methodology and analysis of variance were applied to test the significance of the variables and the acceptability of the nonlinear created model. Finally, a reasonable agreement was found between the experimental results of previous work and predicted modeling results with an average variation of 11%.

Keywords:

specific wear rate, SEM, XRD, response surface methodology, modeling wear rate, high temperature

1. Introduction

There are various types of stainless steel with a wide range of applications. Hence, it is considered the most desirable material, which plays a vital role in most of the manufacturing industries (Suthar et al., 2015), (Sampath, 2015), (Muhammed et al., 2020). Among the stainless steels, austenitic grades are the most commonly used type (Järvenpää et al., 2020), (Subbiah & Rajavel, 2010). They are generally used due to their excellent service performance and low carbon content that results in easy weldability and formability, as well as excellent corrosion resistance (Subbiah & Rajavel,

2010), (Alvi et al., 2020), (Khidhir & Baban, 2019). Among austenitic grades, AISI 304 austenitic stainless steel is the most widely used grade in terms of production and variety of applications such as food industry, medical equipment, biomedical, chemical industry, oil and gas equipment, refineries, construction, and automotive (Alvi et al., 2020), (Maistro, 2018), (Davanageri et al., 2019), (Prajapati & Tiwari, 2021).

When mating surfaces are subjected to rolling or/and sliding motion that results in the removal of asperity from one or both surfaces, this phenomenon is called wear, which leads to a significant loss of material (Prajapati & Tiwari, 2021), (Bhushan, 2013), (Bhaumik et al., 2020). Wear is one of the most common failures that reduce the life of components in applications such as turbine blades, mining machines, and seal valves (Bhaumik et al., 2020), (Li et al., 2019), (Ramya Sree et al., 2020). Wear-related annual economic losses in China amount to 58.47 billion yuan, while the amount in America is 15 billion dollars (Youjun Ye , Jing Li, 2020). As a result, research in the various fields of wear is strongly promoted.

The interfacial temperature in contacting moving parts such as bearings, internal combustion engines, cutting tools, and many other mechanical systems can result from friction or external sources (Dol et al., 2016), (Joseph et al., 2019). In the case of stainless steel, at certain elevated temperatures during the wear process, a hard and glaze oxide layer can form on the worn surfaces, which can reduce debris formation and material removal (M. Wang et al., 2019), (Parthasarathi & Duraiselvam, 2010), (Younes et al., 2020). Many researchers such as (Maistro, 2018), (Chawla et al., 2013), (Singh et al., 2019), (Manohara et al., 2020) studied the influence of applied load and sliding speed on the wear rate of AISI 304 at room temperature. Others such as (M. Wang et al., 2019), (Huang et al., 2020) studied the effect of heat treatment on the wear rate of austenitic stainless steels, and found that a hard oxide layer forms on the surfaces at high temperatures. However, applications at elevated temperatures have recently increased, The study of wear at elevated temperatures for stainless steels has not attracted enough interest (Prajapati & Tiwari, 2021), (Ahmed & Mulapeer, 2021).

Typically, response surface methodology RSM is used as a design of experiment to determine the influence and significance of multiple variables and to develop a numerical model with a minimal number of experiments (Manohara et al., 2020), (Huang et al., 2020). In addition, the central composite design (CCD) method is more commonly used for a nonlinear regression model (Said et al., 2013), (Bashir et al., 2015), (C. N. Wang et al., 2020), (Montgomery, 2009). Similarly, statistical analysis of ANOVA is used to investigate the significance of individual, square, and intersect factors. Therefore, in this work, RSM and CCD methods were used as the design of the experiment then ANOVA analysis was performed to verify the accuracy of the predicted model. Then the experimental and predicted results of six tests were compared to confirm the reality of the mathematical model.

2. Experimental Procedure

The grade austenitic stainless steel of AISI 304 was utilized as a pin in the wear experiment according to the ASTM G99 standard for the wear test of the pin on disc (Method, 2011), while

the super duplex stainless steel AISI 2507 was used as a contoured surface. The chemical composition and mechanical properties of the two alloys are explained in Table 1, and Table 2.

Table 1: Chemical composition and hardness of AISI 304 and AISI 2507 Austenitic and super duplex stainless steels.

Mat.	C	Mn	Pb	S	Si	Cr	Ni	Mo	N	Cu	Fe
AISI 304	0.08	2	0.045	0.03	0.75	18.5	9.3	0	0.1	0	Bal.
AISI 2507	0.03	1.2	0.035	0.02	0.8	25	7.0	3.2	0.27	0.5	Bal.

Table 2: Mechanical properties of alloys AISI 304and AISI 2507.

UNS	Ultimate Strength (Mpa)	Hardness (HV)
AISI 304	766	303
AISI 2507	1146	405

A metallurgical specimen grinder, a furnace, a load carrier, and a temperature controller were prepared as a wear testing machine. The furnace was insulated in all directions to minimize heat transfer to the outlet and to maintain the specific internal temperature. A K-Type thermocouple was used because it has a wide temperature range and high sensitivity (www.rs-online.com, 2018). A temperature controller was used to control the temperature inside the furnace. Figure 1 shows the schematic diagram of the furnace with the dimensions and location of the pin and temperature sensor. A 1000 W circular heater was fixed inside the furnace as the heating source. The temperature sensor was placed inside. Three variables with five levels according to the RSM and CCD method were used to fulfill the orthogonal experiments. The variables and their levels are listed in Table 3.

Table 3: Code and values of wear test parameters of experimental design according to the CCD method

Level	Lowest	Low	Center	High	Highest
Code of CCD variables	-1.6817	-1	0	+1	+1.6817
Temperature/°C	30	140	300	460	570
Load/ N	20	30	45	60	70
Speed/ m/s	0.59	0.89	1.34	1.78	2.08

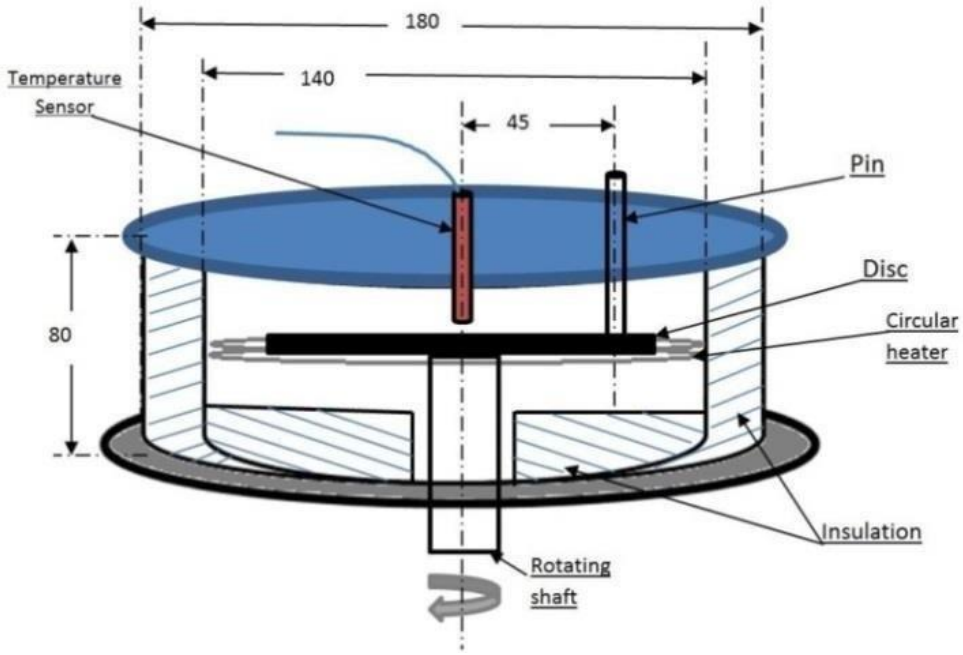

Figure 1: Schematic diagram of insulated furnace containing driving shaft carrying disc and stationary pin with inside thermal control

The tests were carried out under dry conditions with a constant sliding distance of 2000 m. The dimensions of the pins were Ø10 mm and 70 mm in length with a disc diameter of 120 mm and an average active diameter of 90 mm. The face of the pin was polished until surface roughness of 0.4µm and the surface of the disc had a high-quality surface finish. Before each experiment, both parts were cleaned with acetone to remove oil particles or impurities so that contact between them was uniform. The change in pin weight due to wear was measured using a digital balance with an accuracy of 0.0001 g and the rotation speed of the machine was calibrated using a tachometer.

The matrix of complete experimental design with the values of the variables and the order of the experiments according to the CCD, as well as, the results of the experimental volume wear were entered in Table 4. The mass loss was measured and then transferred to the unit volume by dividing the mass loss by the density of austenitic stainless steel of 7.8 g/cm^3. The specific wear rate was determined according to Eq. (1) (Bahshwan et al., 2020), (Davanageri et al., 2018):

$$SWR = \frac{V}{L.S} \qquad (1)$$

Where SWR is the wear rate in $mm^3/N.m$, V is the volume of removal material in mm^3, S is the sliding distance of experiments in m which is constant in this work at 2000 m, and L is applied load in N that is applied vertically at the specimens.

Table 4: The entire experimental matrix according to the CCD, with the results of wear in volume:

Std Order	Temp (°C)	Load (N)	Speed (m/s)	Wear (mm^3)
1	140	30	0.89	11.709
2	460	30	0.89	6.429
3	140	60	0.89	37.653
4	460	60	0.89	11.773
5	140	30	1.78	41.824
6	460	30	1.78	4.196
7	140	60	1.78	84.337
8	460	60	1.78	33.265
9	31	45	1.34	28.406
10	569	45	1.34	2.577
11	300	20	1.34	11.556
12	300	70	1.34	64.298
13	300	45	0.59	9.554
14	300	45	2.08	29.145
15	300	45	1.34	37.219
16	300	45	1.34	36.390
17	300	45	1.34	38.240
18	300	45	1.34	42.589
19	300	45	1.34	38.304
20	300	45	1.34	39.618

3. Results and Discussion

3.1. Influence of Variables on the Specific Wear Rate

Five experiments were conducted at different temperatures and constant applied load and sliding speed of 45 N and 1.34 m/s respectively, to demonstrate the effect of temperature on SWR, as shown in Figure 2. It was observed that the SWR increased with increasing temperature from room temperature to 140°C, then decreased dramatically and reached the minimum at 570°C. Experiments were conducted at 300°C, and 45N, with different sliding speeds, were used to show the effect of sliding speed on SWR, as shown in Figure 3. The SWR increased significantly with increasing sliding speed until it reached 1.78m/s and then decreased slightly. The range of applied load slightly affected the SWR compared with the effect of temperature and sliding speed. Figure 4 shows the effect of applied load on SWR at 300°C, 1.34m/s, and

2000 m. The SWR started high and gradually increased from 2.92 x 10^{-4} mm^3/N.m at 20 N, to 4.70 x 10^{-4} mm^3/N.m at 60 N and then stayed constant until 70 N.

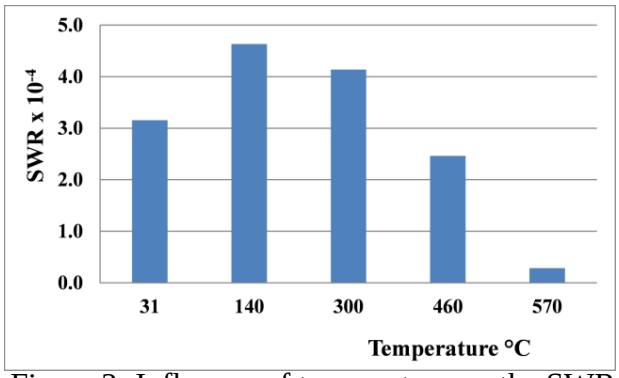

Figure 2: Influence of temperature on the SWR at 45N, 1.34m/s, and 2000 m.

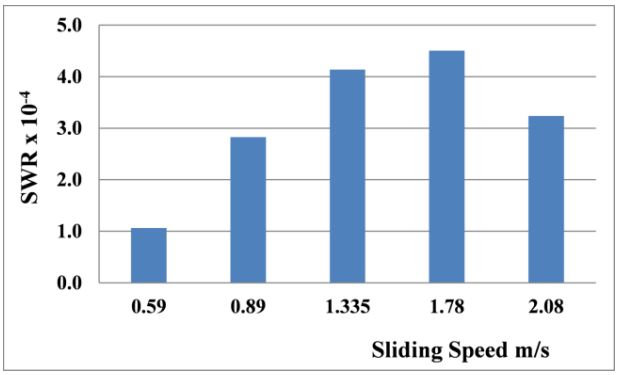

Figure 3: Influence of sliding speed on the SWR at 300°C, 45N, and 2000 m.

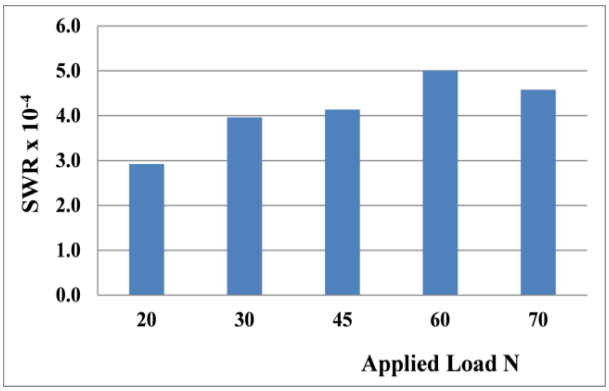

Figure 4: Influence of applied load on the SWR at 300°C, 1.34m/s, and 2000 m.

3.2. SEM and XRD analysis

Surface morphology and the potential oxide formation on the worn surfaces were investigated using scanning electron microscopy (SEM) and X-ray diffraction (XRD). Figs. 5 shows XRD peaks and SEM images of worn surfaces tested at 30°C, with a magnification of 8 KX and 35 KX. Direct grooves and ploughed areas are noticed on the worn surface image of 8 KX, cracks and plastic deformation are noticed in the image with 35 KX. Sever wear occurred on the surfaces tested at 140°C, as shown in Figure 6. Plastic deformation, holes, and cracks with small adhered debris appeared on the surface, while the XRD pattern revealed only original elements. The formation of oxides on the worn surface began at 300°C. Besides the presence of chromium and nickel on the worn surface, the XRD pattern also shows the formation of chromite ($FeCr_2O_4$) and hematite (Fe_2O_3), as shown in Figure 7. N. Parthasarathi

(Parthasarathi & Duraiselvam, 2010) worked on the wear of AISI 316 and observed that oxide formation began at 350°C. The difference may refer to the low applied load that they used compared with this work. On the other hand, in the studies of oxidation of stainless steels, oxide formations occurred at a higher temperature for example X. Huang (Huang et al., 2020) studied the oxidation behavior of austenitic stainless steels and found the oxide formation starts at 800°C. But in wear tests, the friction between the surfaces acts as a source of heat and increases the temperature further than the ambient temperature. The formation of oxide layers increased with increasing temperature and covered a large area of the surface of the sample tested at 460°C, as shown in Figure 8. At 570°C showed in Figure 9, the surface was completely covered by oxide layers, as well as the trace of the sliding wear such as grooves. Oxide layers acted as a solid lubricating material that reduced friction and wears (Parthasarathi & Duraiselvam, 2010). Also, iron oxides and chromium oxides improved surface hardness and enhanced wear resistance (Kazerooni et al., 2011). Therefore, the SWR decreased significantly when the oxide formation on the worn surfaces increased and minimum wear occurred at 570°C.

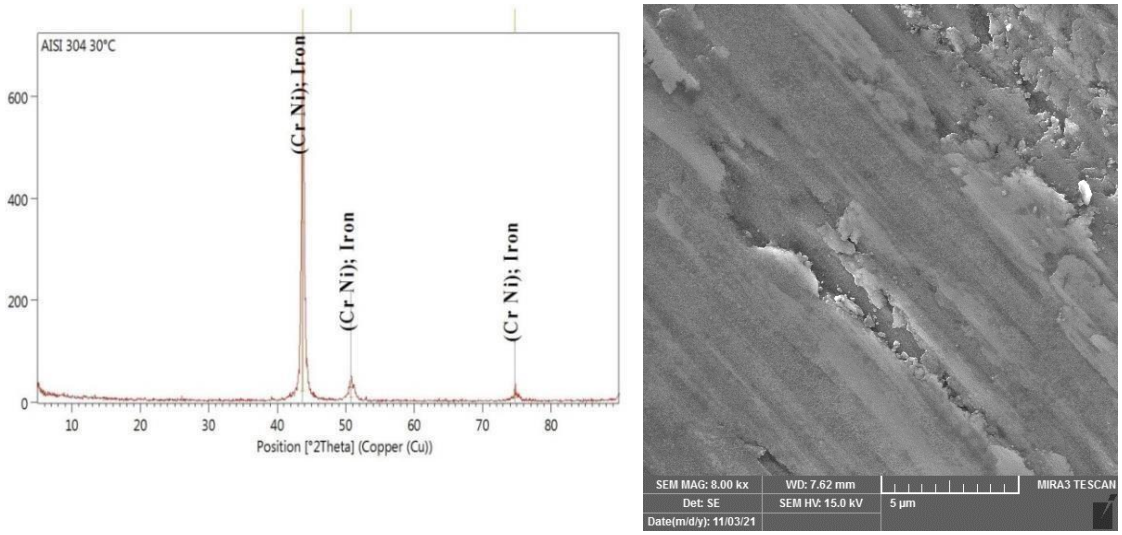

Figure 5: XRD and SEM image of wear tested of AISI 304 at 30°C

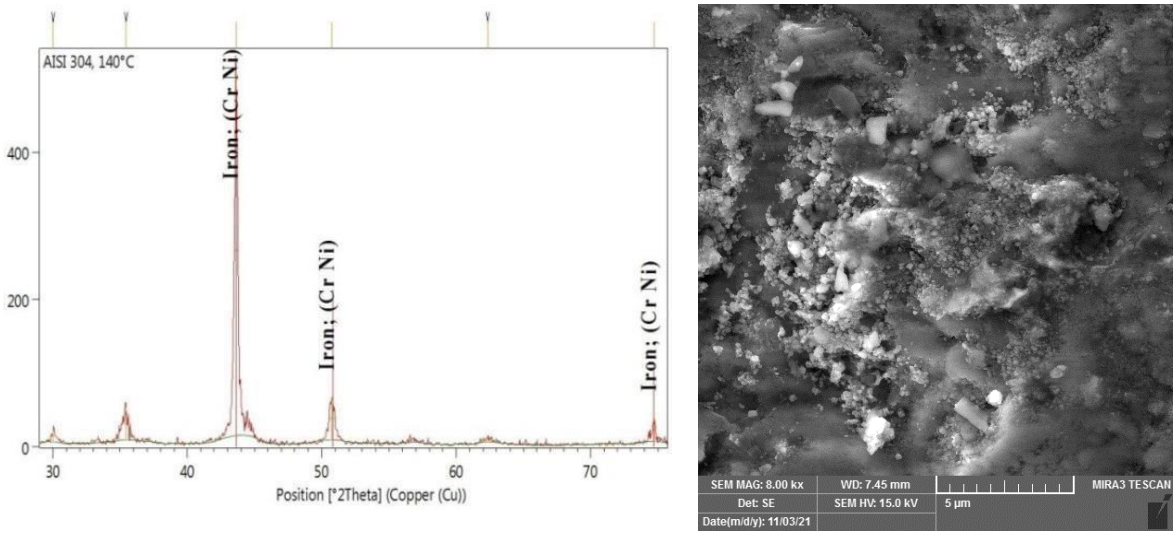

Figure 6: XRD and SEM image of wear tested AISI 304 at 140°C

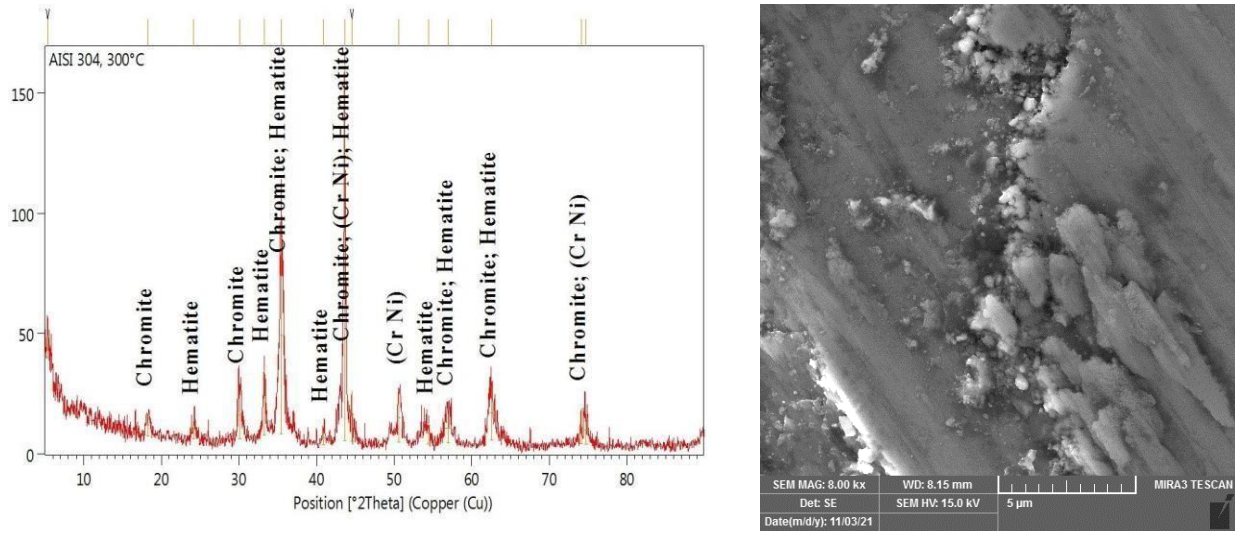

Figure 7: XRD and SEM image of wear tested of AISI 304 at 300°C

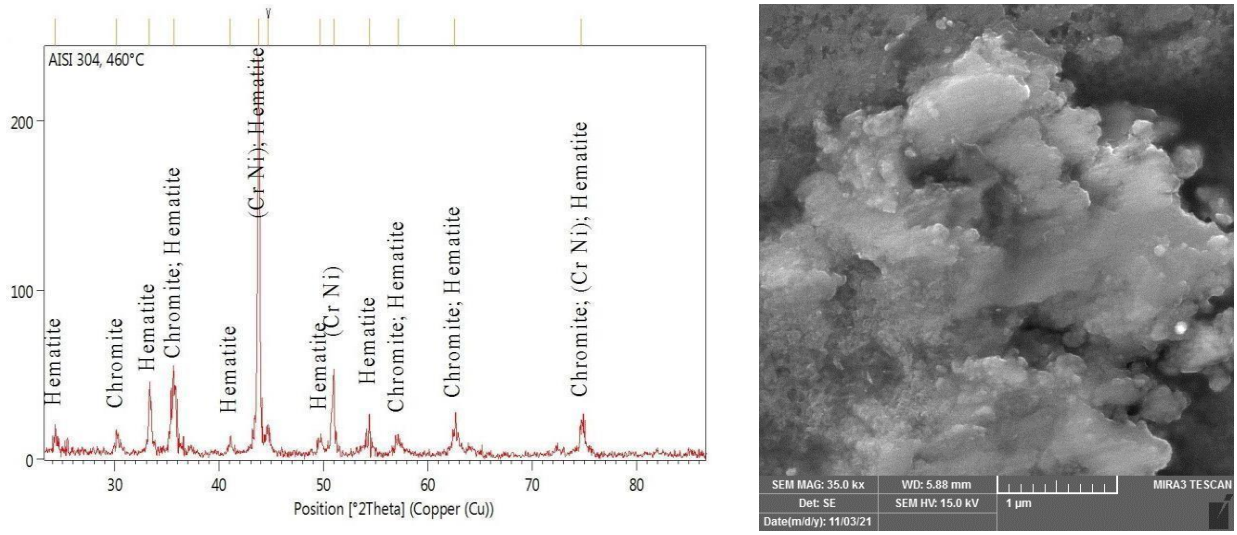

Figure 8: XRD and SEM image of wear tested of AISI 304 at 460°C

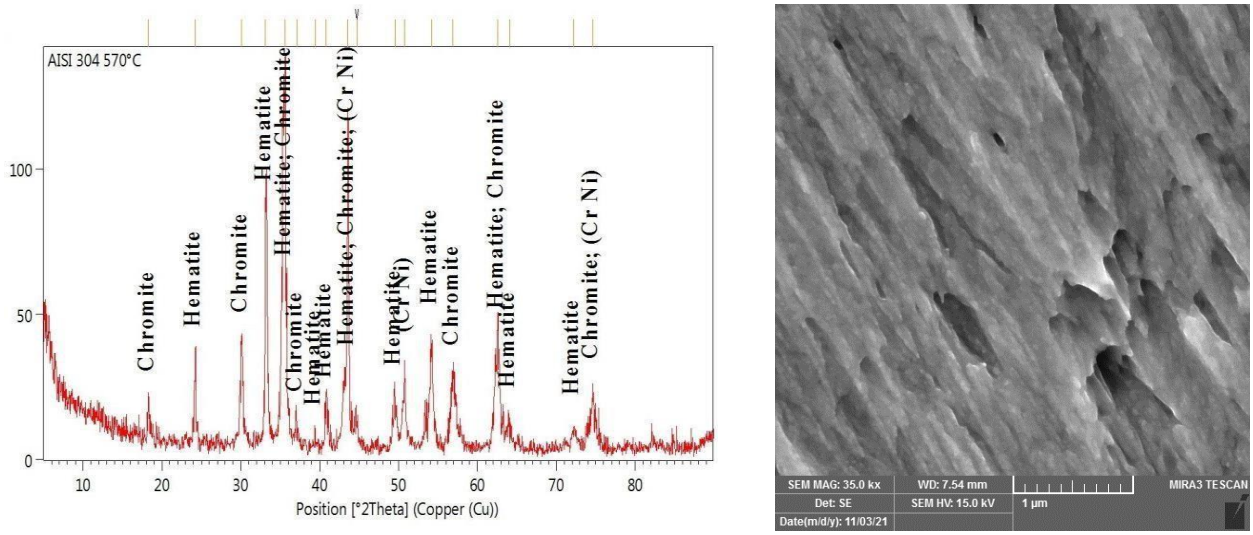

Figure 9: XRD and SEM image wear-tested of AISI 304 at 570°C

3.3. ANOVA Analyses:

To investigate the significance of each parameter and the combined effects on the SWR, the statistical analysis of ANOVA is performed with a 95% confidence interval for SWR. The results of the statistical analysis test are shown in Table 5. The significance of the factors is determined using the p-value. Factors with a p-value of 0.05 or more are considered insignificant, while others with a lower value are considered significant (Mohsin et al., 2020). Single and square terms of temperature and speed were

found to be significant, and the interactions of temperature and speed also had a significant effect on SWR. Single and square terms of load, on the other hand, were insignificant

Table 5: ANOVA analysis for the response surface methodology of SWR x 10^{-4} (mm^3/Nm) versus temperature (T), applied load (L), and sliding speed (S).

Source	DF	P-Value	Contribution%
Model	9	0.001	90.23%
Linear	3	0	60.65%
T	1	0	35.98%
L	1	0.075	3.84%
S	1	0.001	20.82%
Square	3	0.01	19.10%
T*T	1	0.005	12.65%
L*L	1	0.787	0.07%
S*S	1	0.016	8.19%
2-Way Interaction	3	0.055	10.48%
T*L	1	0.757	0.10%
T*S	1	0.009	10.19%
L*S	1	0.665	0.19%
Error	10		9.77%
Lack-of-Fit	5	0.002	9.34%
Pure Error	5		0.43%
Total	19		100.00%

percentage contribution represents the influence ratio of the specific variable on the output variable (Mohsin et al., 2020), (Lian et al., 2020) which is the SWR in this work. The most significant variable that influenced the SWR was temperature, followed by sliding speed and the square of temperature with percentage contribution of 35.98%, 20.82%, and 12.65% respectively. The least contributing factor was the square load, which accounted for only 0.07 percent.

3.4. Modeling of Specific Wear Rate:

A nonlinear model based on the CCD is developed to predict the SWR by examining the experimental data and using Minitab software. The second-order polynomial model includes single, square, and two-factor interactions. The expression of the SWR of AISI 304 austenitic stainless steel is shown to be a nonlinear function, as shown in Equation 2. Due to the importance of accurate prediction of SWR, the insignificant terms must remain in the developed model equation. However, according to the ANOVA analysis, the insignificant parameters show that the SWR is hardly affected by them. The developed model results from the analysis of the RSM and is expressed as follows:

$$SWR \times 10^{-4} = -10.07 + 0.02562.T - 0.016..L + 13.81.S - 0.00003.T^2 - 0.000266.L^2 - 3.16.S^2 + 0.000038.T.L - 0.01315.T.S + 0.0194.L.S \quad (2)$$

3.4.1. Comparison between Experimental and Predicted Results:

To investigate the reality of the developed model, the results of experimental tests of J. Singh (Singh et al., 2019) who studied the wear of AISI 304 used a pin on disc test in various sliding speeds, applied load, and sliding distance, after converting the volumetric wear to SWR, and then compared with the predicted SWR from derived response Eq. (2), as shown in Figure 10. Although the same material and the same type of wear test were used in both papers, the predicted SWR in this paper was slightly higher than the SWR in J. Singh's paper. The difference is due to the different mating surfaces in this work, super duplex AISI 2507 was used, while in other work, a plate made of EN-31 steel was used, which has a lower hardness. The average deviation between predicted SWR according to the model in this work and J. Singh's experimental SWR was 11%.

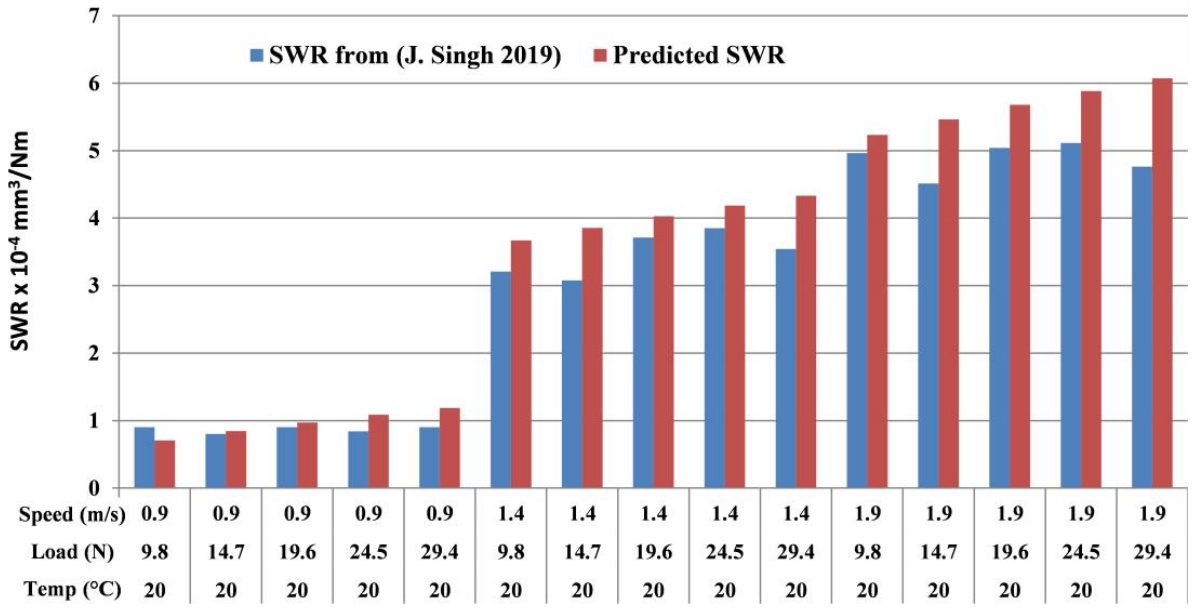

Figure 10. Comparison between predicted SWR with experimental SWR from J. Singh (Singh et al., 2019) of AISI 304 austenitic stainless steel

4. Conclusions

The wear behavior of AISI 304 was investigated at elevated temperatures. In addition, the applied load and sliding speed were used as variable factors in the wear study. Then, the RSM and CCD design of experiment methods were used to study the influence of various factors with an appropriate number of experiments. The morphology of the worn surfaces was illustrated using SEM images, and the composition of the worn surfaces was revealed using XRD analysis. As a result of this work, the following detections and findings were made:

- The SWR of AISI 304 increases linearly with increasing temperature up to 140°C and then decreases dramatically due to the formation of glaze and hard oxide layer that protects the surface from wear and material removal.
- According to the analysis of ANOVA, temperature compared to sliding speed and applied load is the most influential factor on SWR, with an overall contribution of 48%.
- The second factor affecting the SWR is the sliding speed, which peaks at 1.6 m/s and then steadily decreases. The SWR increases linearly but slightly with increasing applied load, with a minimal contribution of only 7%.

- Images from SEM show that deep grooves, ploughs, and cracks appear at low temperatures and disappear or decrease at higher temperatures.
- The results of the XRD analysis show that the formation of hematite and chromite on the worn surfaces starts at 300°C and increases with increasing temperature.
- When compared to other experimental results, a created equation model for predicting SWR of AISI 304 demonstrated good acceptability.

References

Ahmed, D. A., & Mulapeer, M. M. (2021). Modeling Wear Rate of Super Austenitic Stainless Steel S31254 at Elevated Temperature by Response Surface Methodology. Design Engineering (TORONTO), 8, 4334–4348.

Alvi, S., Saeidi, K., & Akhtar, F. (2020). High temperature tribology and wear of selective laser melted (SLM) 316L stainless steel. Wear, 448–449(January), 203228. https://doi.org/10.1016/j.wear.2020.203228

Bahshwan, M., Myant, C. W., Reddyhoff, T., & Pham, M. S. (2020). The role of microstructure on wear mechanisms and anisotropy of additively manufactured 316L stainless steel in dry sliding. Materials and Design, 196, 109076. https://doi.org/10.1016/j.matdes.2020.109076

Bashir, M. J. K., Amr, S. S. A., Aziz, S. Q., Choon Aun, N., & Sethupathi, S. (2015). Wastewater Treatment Processes Optimization Using Response Surface Methodology (RSM) Compared with Conventional Methods: Review and Comparative Study. Middle-East Journal of Scientific Research, 23(2), 244–252. https://doi.org/10.5829/idosi.mejsr.2015.23.02.52

Bhaumik, S., Mukherjee, M., Sarkar, P., Nayek, A., & Paleu, V. (2020). Microstructural and wear properties of annealed medium carbon steel plate (EN8) cladded with martensitic stainless steel (AISI410). Metals, 10(7), 1–16. https://doi.org/10.3390/met10070958

Bhushan, B. (2013). Introduction to tribology (Second Edi). John Wiley & Sons.

Chawla, K., Saini, N., Dhiman, R., & Engineering, C. (2013). Investigation of tribological behavior of stainless steel 304 and grey cast iron rotating against EN32 steel using pin on disc apparatus. IOSR Journal of Mechanical, 9(4), 18–22.

Davanageri, M. B., Narendranath, S., & Kadoli, R. (2018). Finite Element Wear Behaviour Modeling of Super duplex stainless steel AISI 2507 Using Ansys. IOP Conference Series: Materials Science and Engineering, 376(1). https://doi.org/10.1088/1757-899X/376/1/012131

Davanageri, M. B., Narendranath, S., & Kadoli, R. (2019). Modeling and Optimization of Wear Rate of AISI 2507 Super Duplex Stainless Steel. Silicon, 11(2), 1023–1034.

Dol, T. S., Dhole, A. B., Mahamuni, T. M., & Kumbhar, N. A. (2016). Review of Developments in Pin-

On-Disc Tribometer for Environment Control. 4(Ix), 452–459.

Huang, X., Xiao, K., Fang, X., Xiong, Z., Wei, L., Zhu, P., & Li, X. (2020). Oxidation behavior of 316L austenitic stainless steel in high temperature air with long-term exposure. Materials Research Express, 7(6). https://doi.org/10.1088/2053-1591/ab96fa

Järvenpää, A., Jaskari, M., Kisko, A., & Karjalainen, P. (2020). Processing and properties of reversion- treated austenitic stainless steels. Metals, 10(2). https://doi.org/10.3390/met10020281

Joseph, J., Haghdadi, N., Shamlaye, K., Hodgson, P., Barnett, M., & Fabijanic, D. (2019). The sliding wear behaviour of CoCrFeMnNi and AlxCoCrFeNi high entropy alloys at elevated temperatures. Wear, 428–429(February), 32–44. https://doi.org/10.1016/j.wear.2019.03.002

Kazerooni, N. A., Bahrololoom, M. E., Shariat, M. H., Mahzoon, F., & Jozaghi, T. (2011). Effect of ringer's solution on wear and friction of stainless steel 316L after plasma electrolytic nitrocarburising at low voltages. Journal of Materials Science and Technology, 27(10), 906–912. https://doi.org/10.1016/S1005-0302(11)60163-1

Khidhir, G. I., & Baban, S. A. (2019). Efficiency of dissimilar friction welded 1045 medium carbon steel and 316L austenitic stainless steel joints. Journal of Materials Research and Technology, 8(2), 1926–1932. https://doi.org/10.1016/j.jmrt.2019.01.010

Li, L., Zhao, S., Zhang, N., Guo, Y., & Gan, H. (2019). Enhanced Wear Resistance of Iron-Based Alloy Coating Induced by Ultrasonic Impact. Coatings, 804(9), 1–14.

Lian, G., Zhao, C., Zhang, Y., Feng, M., & Jiang, J. (2020). Investigation intomicro-hardness and wear resistance of 316L/SiC composite coating in laser cladding. Applied Sciences (Switzerland), 10(9). https://doi.org/10.3390/app10093167

Maistro, G. (2018). Low-temperature carburizing / nitriding of austenitic stainless steels Influence of alloy composition on microstructure and properties. CHALMERS UNIVERSITY OF TECHNOLOGY Gothenburg, Sweden.

Manohara, H. R., Thipperudrappa, N., Basava, & Thippeshappa, S. (2020). Influence of titanium carbide and activated carbon particles on the wear, mechanical properties and microstructure study of a413 metal matrix composite. Indian Journal of Engineering and Materials Sciences, 27(4), 952–958.

Method, S. T. (2011). Standard Test Method for Wear Testing with a Pin-on-Disk Apparatus 1. Wear, 05(Reapproved 2010), 1–5. https://doi.org/10.1520/G0099-05R10.2

Mohsin, I., He, K., Li, Z., Zhang, F., & Du, R. (2020). Optimization of the Polishing Efficiency and Torque by Using Taguchi Method and ANOVA in Robotic Polishing. Applied Sciences, 10, 2–15. https://doi.org/10.3390/app10030824

Montgomery, D. C. (2009). Introduction To Statistical Quality Control. In J. Welter (Ed.), John Wiley

& Sons (Sixth edit). Don Fowley, Daniel Sayer. https://doi.org/10.2307/2988304

Muhammed, M., Mustapha, M., Ginta, T. L., Ali, A. M., Mustapha, F., & Hampo, C. C. (2020). Statistical review of microstructure-property correlation of stainless steel: Implication for preand post-weld treatment. Processes, 8(7). https://doi.org/10.3390/pr8070811

Parthasarathi, N. L. ., & Duraiselvam, M. (2010). Improvement of High Temperature Wear Resistance of AISI 316 ASS through NiCrBSiCFe Plasma Spray Coating. Journal of Minerals and Materials Characterization and Engineering, 09(07), 653–670. https://doi.org/10.4236/jmmce.2010.97047

Prajapati, D. K., & Tiwari, M. (2021). The correlation between friction coefficient and areal topography parameters for AISI 304 steel sliding against AISI 52100 steel. Friction, 9(1), 41–60. https://doi.org/10.1007/s40544-019-0323-1

Ramya Sree, K., Keerthi Reddy, G., Aishwarya, K., Nirmala Devi, E., & Subbiah, R. (2020). New Insights of Wear Behavior Analysis on Low Temperature Treated AISI 253MA Stainless steel Material by Gas Nitriding Process. E3S Web of Conferences, 184. https://doi.org/10.1051/e3sconf/202018401003

Said, M. S., Ghani, J. A., Kassim, M. S., Tomadi, S. H., Hassan, C., Haron, C., & Kedah, K. (2013). Comparison between Taguchi Method and Response Surface Methodology (RSM) In Optimizing Machining Condition. International Conference on Robust Quality Engineering, 60–64. https://core.ac.uk/download/pdf/235641908.pdf

Sampath, P. S. (2015). Wear and Corrosion Studies on Ferritic Stainless Steel (Ss 409M). International Journal of Research in Engineering and Technology, 04(04), 502–511. https://doi.org/10.15623/ijret.2015.0404088

Singh, J., Sharma, S., & Singh, A. P. (2019). Oxidation Effects on wear Resistance of SS-304 and SS-316 Austenitic Stainless Steels. International Journal of Innovative Technology and Exploring Engineering (IJITEE), 8(10), 2353–2357.

Subbiah, R., & Rajavel, R. (2010). Dry sliding wear behaviour analysis of nitrided 316LN grade austenitic stainless steels using gas nitriding process. Journal of Theoretical and Applied Information Technology, 19(2), 98–101.

Suthar, F., Puntambekar, U., Joshi, M., & Daspujari, R. (2015). Comparative Evaluation of Abrasive Wear Resistance of Various Stainless Steel Grades. Ge-IInternational Journal of Engineering Research, 3(7), 20–35.

Wang, C. N., Nguyen, N. A. T., & Dang, T. T. (2020). Solving order planning problem using a heuristic approach: The case in a building material distributor. Applied Sciences (Switzerland), 10(24), 1–21. https://doi.org/10.3390/app10248959

Wang, M., Wang, Y., Liu, H., Wang, J., & Yan, F. (2019). Interrelated effects of temperature and load

on fretting behavior of SAF 2507 super duplex stainless steel. Tribiology International, 136(March), 140–147. https://doi.org/10.1016/j.triboint.2019.03.042

www.rs-online.com. (2018). Thermocouple Selection Guide. https://docs.rs-online.com/96d5/0900766b815e5302.pdf

Youjun Ye , Jing Li, X. L. and L. L. (2020). Study on Failure Mechanism and Phase Transformation of 304 stainless steel during erosion wear. Metals, 10(1427), 15. https://doi.org/10.3390/met10111427

Younes, A., Nnamchi, P., Medina, J., Pérez, P., Villapún, V. M., Badimuro, F., Kamnis, S., Jimenez-Melero, E., & González, S. (2020). Wear rate at RT and 100 °C and operating temperature range of microalloyed Cu50Zr50 shape memory alloy. Journal of Alloys and Compounds, 817. https://doi.org/10.1016/j.jallcom.2019.153330